Electronic correlations in coherent transport through a two quantum dot system

Bogdan R. Bułka[1] and Tomasz Kostyrko[2]
[1]*Institute of Molecular Physics, Polish Academy of Sciences, ul. M. Smoluchowskiego 17, 60-179 Poznań, Poland*
[2]*Institute of Physics, A. Mickiewicz University, ul. Umultowska 85, 61-614 Poznań, Poland*
(Received 1 March 2004; published 23 November 2004)

Coherent electronic transport through a double quantum dot (2qd) system connected in a series with electrodes is studied by means of nonequilibrium Green functions and using the equation of motion method, in which all electron correlations in the 2qd are treated exactly. For moderate Coulomb interactions we predict features in a conductance characteristics resulting from transmission through triplet states, which can be strongly activated for larger source-drain voltages. The analysis of the spin-spin correlation functions shows strong antiferromagnetic correlations arising from transport through the singlet state and a reduction of the total magnetic moment. However, when the transmission channel corresponding to the triplet state becomes activated the antiferromagnetic correlations are much weaker, the spins behave as free electrons spins and strongly fluctuate. We speculate that this effect can be seen in wide range of a gate voltage for a double electron occupancy of the 2qd.

DOI: 10.1103/PhysRevB.70.205333 PACS number(s): 73.63.Kv, 73.21.La, 71.10.−w

I. INTRODUCTION

Recent spectacular advances in nanotechnology gave possibility to experimental studies of coherent transport in quantum dots,[1–3] carbon nanotubes,[4,5] quantum corrals,[6] and single molecules.[7,8] It was possible to investigate an interplay of interference processes and electron correlations, and their influence on transport characteristics. An interesting idea of the last decade was constructing a qubit, due to which one could coherently manipulate on entanglement electron pairs and which could be used for a quantum computing.[9] Therefore, many experimental efforts were undertaken to build coherently coupled quantum dot devices. A simplest realization was a two quantum dot system connected with the source and the drain electrodes either in parallel[10–13] or in series.[14–18] Such a system contains only a few interacting electrons, which can form many-body singlet and triplet states. Coherent coupling of these states with conducting electrons leads to the Kondo resonance,[2,3] which involves both the orbital and spin degree of freedom of electrons.[19]

In this paper we want to study theoretically coherent transport through the system of two-quantum dots (2qd) connected in series. The problem is complex and one needs approximations to deal with both intra- and interdot Coulomb interactions as well as the coupling between the dots and the macroscopic electrodes. The one-particle approximations for the interactions[20–22] and the perturbative treatment of the Coulomb interactions[23] allows one to treat exactly the coupling to the electrodes. However, these methods are justified only in the limit of weak interactions, relatively strong lead-dot coupling, and low temperatures. If Coulomb interactions are strong enough, one can adapt the slave boson method, in which the energy levels are assumed to be occupied by only single electron.[24–27] Usually one applies the mean-field approximation (SBMFA), which reduces the many-body problem to the one-particle one with constraints. It was shown that SBMFA takes into account spin fluctuations and can be applied for low temperatures.[28] Since charge fluctuations are neglected, applicability of SBMFA is restricted to the limit of small source-drain voltages. Important effects of correlations and formation of many-particle states are outside the scope of these approaches.

A role of many-particle states in transport through the 2qd system were studied in the incoherent sequential tunneling regime, which usually implies the perturbative treatment of the electrode-dot coupling (see, for example, Refs. 29–35). However, in this conduction regime important aspects of interference processes are ignored. Just recently Aguado and Langreth[36] studied coherent transport in the 2qd system using a generalization of the noncrossing approximations for large intradot Coulomb interactions. They predicted a smooth transition from a state of two isolated impurities to a coherent superposition of the many-body states of each dot when the interdot electron hopping increases.

In this paper we want to consider a problem of electronic correlations and a role of many-particle states in coherent transport in the 2qd system. An interesting issue seems to be interplay of transmission channels through the singlet and the triplet state. This aspect has been studied recently for the Kondo model showing on effects closed to the singlet-triplet degeneracy.[37–40] The approach required a spin $S=1$ ground state in a quantum dot and took into account spin fluctuations, neglecting charge fluctuations. Our 2qd system will be described by the two-impurity Anderson model and the equation of motion (EOM) approach will be used, within which charge fluctuations are taken into account. The EOM with various approximate decoupling procedures for the higher order Green functions was used in previous papers.[41–43] The disadvantage of these procedures lies in omitting higher order correlation functions and neglecting a contribution to transport from transmission channels through excited states. In the present paper we apply the procedure, which treats all electronic correlations exactly within the 2qd system and requires determination of various intra- and interdot correlation functions, which are computed here in a fully self-consistent way. In our decoupling some higher order correlations between electrons at the 2qd and conducting electrons from the

electrodes are omitted, which is justified above the temperatures typical of the Kondo effect.

We analyze in detail the differential conductance of the 2qd system as well as some relevant intra- and interdot correlation functions in both the equilibrium limit and in the nonequilibrium case. For the intermediate values of the Coulomb repulsion the conductance shows some structure, disregarded in the previous papers, which is due to the dynamic occupation of the triplet excited states of the double occupied 2qd. This structure is accompanied with changes of the total magnetic moment, which is also due to the existence of the triplet states. Although the structure in the conductance is best visible at low temperatures, it should be detectable in a wide temperature range. The computations made for the finite values of the source-drain voltage show significant changes in the differential conductance, some transmission channels corresponding to excited states become strongly activated. We find a reduction of spin-spin correlations, which is due to voltage induced charge fluctuations.

The plan of our paper is as follows. In Sec. II we introduce the Hamiltonian of the system and present the basic formulas of the nonequilibrium Green functions theory used here to compute the current. This section includes also details of our decoupling of a set of equations for the Green functions. The results of the numerical computations of the transport properties and the correlation functions are presented in Sec. III. The paper concludes with a summary in Sec. IV.

II. DESCRIPTION OF THE SYSTEM AND DETERMINATION OF THE CURRENT

Our model for the 2qd connected in series to the electrodes is given by the three part Hamiltonian $H=H_{2\mathrm{qd}}+H_{2\mathrm{qd\text{-}el}}+H_{\mathrm{el}}$. The 2qd system is described by the Hubbard Hamiltonian

$$H_{2\mathrm{qd}}=\sum_{i,\sigma}\epsilon_i n_{i,\sigma}+t_{12}\sum_{\sigma}(c^{\dagger}_{1,\sigma}c_{2,\sigma}+c^{\dagger}_{2,\sigma}c_{1,\sigma})+\frac{U_0}{2}\sum_{i,\sigma}n_{i,\sigma}n_{i,-\sigma}+U_1\sum_{\sigma,\sigma'}n_{1,\sigma}n_{2,\sigma'}, \tag{1}$$

where the first term gives a local electron potential energy, in which only one energy level ϵ_i for each quantum dot is taken into account—it means that the energy level separation $\Delta\epsilon$ is very large, larger than the other parameters. The second term corresponds to an electron transfer between the quantum dots, which is proportional to the hopping integral t_{12}. Two last terms describe Coulomb interactions for electrons on the quantum dot and interdot interactions, where the parameters U_0 and U_1 are the intra- and the interdot coulombic integrals, respectively. The Hamiltonian

$$H_{2\mathrm{qd\text{-}el}}=t_L\sum_{k,\sigma}(c^{\dagger}_{kL,\sigma}c_{1,\sigma}+c^{\dagger}_{1,\sigma}c_{kL,\sigma})+t_R\sum_{k,\sigma}(c^{\dagger}_{kR,\sigma}c_{2,\sigma}+c^{\dagger}_{2,\sigma}c_{kR,\sigma}) \tag{2}$$

corresponds to the coupling of the 2qd system with the left (L) and the right (R) electrode. Electrons in the electrodes ($\alpha=L,R$) are described by

$$H_{\mathrm{el}}=\sum_{k,\alpha,\sigma}\epsilon_{k\alpha}c^{\dagger}_{k\alpha,\sigma}c_{k\alpha,\sigma}. \tag{3}$$

Although in this work we describe the situation in the system of quantum dots the same model can be used for transport through a two atomic molecules.

The current is calculated from the time evolution of the occupation number $n_L=\Sigma_{k,\sigma}c^{\dagger}_{kL,\sigma}c_{kL,\sigma}$ for electrons in the left electrode

$$I\equiv -e\left\langle\frac{dn_L}{dt}\right\rangle=\frac{ie}{\hbar}\left[\sum_{k,\sigma}t_L\langle c^{\dagger}_{kL,\sigma}c_{1,\sigma}\rangle-\mathrm{c.c.}\right]. \tag{4}$$

Using the nonequilibrium Greens functions[44,45] one can rewrite this formula to the form

$$I=\frac{e}{h}\sum 2i\Gamma_L\int d\omega\{f_L(\omega)2i\,\mathrm{Im}[\langle\langle c_{1,\sigma}|c^{\dagger}_{1,\sigma}\rangle\rangle^{a}_{\omega}]-\langle\langle c_{1,\sigma}|c^{\dagger}_{1,\sigma}\rangle\rangle^{<}_{\omega}\}. \tag{5}$$

Here, $\Gamma_\alpha=\pi\rho_\alpha t^2_\alpha$ corresponds to the electron transfer rate between the 2qd system and the α electrode, the electron density of states in the electrodes is assumed to be constant ρ_α near the Fermi level. $f_\alpha(\omega)$ denotes the Fermi-Dirac distribution function for electrons in the α electrode with the chemical potential μ_α. We use the notation $\langle\langle c_{1\sigma}|c^{\dagger}_{1\sigma}\rangle\rangle$ with the superscript a, r, and $<$ for the advance, the retarded, and the lesser Green function. The formula (5) is exact, no approximations have been done. The main problem is to determine the Green functions, which can be performed within an approximate method only.

In order to study the current (5), one has to determine the lesser Green function $\langle\langle c_{1,\sigma}|c^{\dagger}_{1,\sigma}\rangle\rangle^{<}_{\omega}$ for a nonequilibrium situation with the stationary charge flow. The procedure is similar to that one used in derivation of the quantum Boltzmann equation and the Wigner function.[44,46,47] Let us consider the time dependent Green function $\langle\langle a(t)|b(t')\rangle\rangle^{<}$, where a and b are products of annihilation and creation operators for electrons at the 2qd system. Since we are interested in the stationary current the time transformation is used: $\tau=t-t'$ and $t_0=(t+t')/2$. The derivative of the Green function with respect to t_0 should be equal to zero and with respect to τ:

$$i\frac{\partial}{\partial\tau}\langle\langle a(t_0+\tau/2)|b(t_0-\tau/2)\rangle\rangle^{<}=\frac{i}{2}\left[\left\langle\left\langle\frac{\partial}{\partial\tau}a(t_0+\tau/2)\middle|b(t_0-\tau/2)\right\rangle\right\rangle^{<}-\left\langle\left\langle a(t_0+\tau/2)\middle|\frac{\partial}{\partial\tau}b(t_0-\tau/2)\right\rangle\right\rangle^{<}\right]. \tag{6}$$

Therefore, the Fourier transform of the lesser Green function is expressed as

$$\langle\langle a|b\rangle\rangle_\omega^< \equiv \int d\tau e^{i\omega\tau}\langle\langle a(t_0+\tau/2)|b(t_0-\tau/2)\rangle\rangle^< = \frac{1}{2}[((a|b\rangle\rangle_\omega^< - \langle\langle a|b))_\omega^<], \quad (7)$$

where $((a|b\rangle\rangle_\omega^<$ and $\langle\langle a|b))_\omega^<$ are auxiliary functions defined as

$$\omega((a|b\rangle\rangle_\omega^< = i\int d\tau e^{i\omega\tau}\left\langle\left\langle \frac{\partial}{\partial\tau}a(t_0+\tau/2)\middle| b(t_0-\tau/2)\right\rangle\right\rangle^< \quad (8)$$

$$\omega\langle\langle a|b))_\omega^< = i\int d\tau e^{i\omega\tau}\left\langle\left\langle a(t_0+\tau/2)\middle| \frac{\partial}{\partial\tau}b(t_0-\tau/2)\right\rangle\right\rangle^<. \quad (9)$$

(Note the different bracket notation used for both the functions.) In order to find $\langle\langle a|b\rangle\rangle_\omega^<$ one has first to determine $((a|b\rangle\rangle_\omega^<$ from a series of equation of motions with respect to the first operator a (e.g., following the scheme presented by Niu *et al.*);[48] and next—the second function $\langle\langle a|b))_\omega^<$ (repeating the equation of motion procedure with respect to the second operator b). The physical quantities calculated by means of the lesser Green functions fulfill the quantum reciprocity relations (i.e., the Onsager's reciprocity theorem for nonequilibrium quantum physics). Our approach is equivalent to the Dyson equation approach presented by Haug and Jauho (see Chap. 8.2 in Ref. 44).

In the absence of the coupling to the leads, the sequence of equations of motion for the Green functions is closed and they can be determined exactly for any values of the interdot hopping t_{12}, local energy values ϵ_i, and the interaction parameters, U_0, U_1. For the finite coupling to the leads, many mixed Green functions involving both the leads and the 2qd degrees of freedom, enter the system of equations of motion, and they have to be included in an approximate way. The coupling to the electrodes is treated here to lowest order with respect to the electron transfer rate Γ_α. We assume that

$$\sum_k ((c_{kL,\sigma}a|c_{i,\sigma}^\dagger\rangle\rangle^< \approx t_L g_L^r((c_{1,\sigma}a|c_{i,\sigma}^\dagger\rangle\rangle^< + t_L g_L^<\langle\langle\, c_{1,\sigma}a|c_{i,\sigma}^\dagger)\rangle\rangle^a, \quad (10)$$

$$\sum_k \langle\langle c_{kL,\sigma}a|c_{i,\sigma}^\dagger\rangle\rangle^a \approx t_L g_L^a\langle\langle c_{1,\sigma}a|c_{i,\sigma}^\dagger\rangle\rangle^a, \quad (11)$$

where a is a product of operators for electrons at the 2qd system, and the equivalent approximations are made for the terms including the coupling with the right electrode. The higher order correlation processes for the electron transfer between the electrodes and the 2qd system are omitted (see the Appendix, in which the approach is presented for the case of the single dot). In this way we neglect processes leading to the Abrikosov-Suhl resonance and the Kondo effect. On the other hand, charge fluctuation and all correlations in the 2qd system are included. The results are reliable for temperatures higher than the Kondo temperature T_K. Note, however, that our procedure takes into account all electronic correlations in the 2qd system and in the limit of the vanishing coulomb interactions it leads to exact results for the Green functions for any value of dot-lead coupling, arbitrary temperature, and the bias voltage.

Through the series of equations of motion, the one-particle Green functions are coupled with many-particle Green functions. The highest order Green functions are of the type: $\langle\langle c_{1,\sigma}n_{2,\sigma}n_{1,-\sigma}n_{2,-\sigma}|c_{i,\sigma}^\dagger\rangle\rangle$. The Green functions depend on the Hamiltonian parameters and on the correlators. For a paramagnetic case one can distinguish 19 correlators: $\langle n_{1,\sigma}\rangle$, $\langle c_{1,\sigma}^\dagger c_{2,\sigma}\rangle$, $\langle n_{1,\sigma}n_{2,-\sigma}\rangle$, $\langle n_{1,\sigma}n_{1,-\sigma}n_{2,-\sigma}\rangle$, $\langle c_{1,\sigma}^\dagger c_{2,\sigma}c_{1,-\sigma}^\dagger c_{2,-\sigma}\rangle$, $\langle n_{1,\sigma}n_{1,-\sigma}n_{2,\sigma}\rangle$, $\langle c_{1,\sigma}^\dagger c_{2,\sigma}n_{1,-\sigma}n_{2,-\sigma}\rangle$, etc. In general the correlators are determined by means of the lesser Green functions, for example

$$\langle n_{1,\sigma}n_{2,-\sigma}\rangle = \int \frac{d\omega}{2\pi i}\langle\langle c_{1,\sigma}n_{2,-\sigma}|c_{1,\sigma}^\dagger\rangle\rangle_\omega^<, \quad (12)$$

where the lesser Green function is symmetrized, as in Eq. (7). Since the Green functions depend on the correlators, one gets a set of 19 self-consistent integral equations. We use a spectral decomposition procedure, in which any physical quantity is written as a sum of contributions corresponding to electron transitions between any energy state in the system. In our approximation the poles of the Green functions are expressed as differences of energy eigenvalues $E_\lambda(N)$ of the isolated 2qd corresponding to different electron occupation N and shifted by the factor determined by the coupling to the leads $i\Gamma_\alpha$. The Green functions are decomposed into partial fractions and the integrals are calculated analytically (see also the Appendix). In this way a set of 19 self-consistent integral equations is reduced to a set of 19 linear equations. Solving numerically this set of equations we find all correlators. Finally, one calculates the one-particle lesser and advanced Green functions and from the formula (5) the current.

The many-particle correlators can be expressed by different Green functions. For example, $\langle n_{1,\sigma}n_{2,-\sigma}\rangle$ can be calculated by means of the Green function $\langle\langle c_{1,\sigma}n_{2,-\sigma}|c_{1,\sigma}^\dagger\rangle\rangle_\omega^<$ as well as $\langle\langle c_{2,-\sigma}n_{1,\sigma}|c_{2,-\sigma}^\dagger\rangle\rangle_\omega^<$. We have checked that the results presented later do not depend on the choice of the Green functions used in the calculations of the correlators.

III. TRANSPORT THROUGH TWO-QUANTUM DOT SYSTEM

A. Zero-voltage conductance

Lets us first apply the procedure described earlier for small voltages ($V\to 0$). In this case one can use the equilibrium Green functions, which poles correspond to energies of the isolated two-quantum dot system with $N=1$, 2, 3, and 4 electrons. Table I summarizes the energy structure for $\epsilon_1=\epsilon_2$ (see, e.g., Ref. 49 for details). In our studies a strong electron transfer between the quantum dots is assumed $t_{12}>\Gamma_\alpha$, and the moderate values for the coulomb interaction parameters are taken: the intradot coulomb integral $U_0=6$ and the interdot coulomb integral $U_1=1.6$ (with respect to the hopping integral treated as the unity $t_{12}=1$). The results are presented in Fig. 1 for the temperature $T=0$ and $\epsilon_1=\epsilon_2$. One can see four conductance peaks of the height

TABLE I. States, eigenvalues, and the ground states energy of the isolated two-quantum dot system for $\epsilon_1=\epsilon_2$. Below we put $\Delta=\sqrt{16t_{12}^2+(U_0-U_1)^2}$.

State	Eigenvalue	Ground state energy
0 electron		0
$\|0,0\rangle$	0	
1 electron		$\epsilon_1-\|t_{12}\|$
$1/\sqrt{2}\,(\|\sigma,0\rangle\pm\|0,\sigma\rangle)$	$\epsilon_1\pm t_{12}$	
2 electron		$2\epsilon_1+\frac{1}{2}(U_0+U_1-\Delta)$
$\|+,+\rangle$		
$1/\sqrt{2}\,(\|+,-\rangle-\|-,+\rangle)$	$2\epsilon_1+U_1$	
$\|-,-\rangle$		
$\alpha/\sqrt{2}\,(\|+,-\rangle+\|-,+\rangle)$ + $\beta/\sqrt{2}\,(\|2,0\rangle+\|0,2\rangle)$	$2\epsilon_1+\frac{1}{2}(U_0+U_1\pm\Delta)$	
$1/\sqrt{2}\,(\|2,0\rangle-\|0,2\rangle)$	$2\epsilon_1+U_0$	
3 electron		$3\epsilon_1+U_0+2U_1-\|t_{12}\|$
$1/\sqrt{2}\,(\|2,\sigma\rangle\pm\|\sigma,2\rangle)$	$3\epsilon_1+U_0+2U_1\pm t_{12}$	
4 electron		$4\epsilon_1+2U_0+4U_1$
$\|2,2\rangle$	$4\epsilon_1+2U_0+4U_1$	

$\sim(2e^2/h)\times 0.6$. Comparing the ground state energies $E_g(N+1)=E_g(N)$ one finds the position of the conductance peaks: (1) $\epsilon_1-E_F=|t_{12}|$, (2) $\epsilon_1-E_F=-|t_{12}|-(U_0+U_1-\Delta)/2$, (3) $\epsilon_1-E_F=|t_{12}|-(U_0+3U_1+\Delta)/2$, and (4) $\epsilon_1-E_F=-|t_{12}|-U_0-2U_1$, where $\Delta=\sqrt{16t_{12}^2+(U_0-U_1)^2}$. The bottom part of Fig. 1 shows the average number of electrons $\langle n_{1,+}\rangle$ (the solid curve), which increases at these points. It means that the resonant conductance peaks correspond to energy levels, for which an extra electron is introduced to the system. The results exhibit the electron-hole symmetry (seen in the conductance spectrum as well as in the correlators). For our case the symmetry point is in the middle of the Hubbard gap at $\epsilon_1-E_F=-U_0/2-U_1=-4.6$. Our further analysis will be therefore restricted to the half of the electronic structure.

Similar four peak conductance characteristics can be found in the literature.[41–43] In the present case the peaks are much higher, which is related to our procedure. Usually many-particle Green functions were decoupled to one- and two-particle Green functions in order to close the set of self-consistent equations.[41–43] The decoupling approximation introduced some dissipation processes, which resulted in a reduction of the conductance peaks. In our procedure all many-particle Green functions on the 2qd system are taken into account and transitions between many-particle states are treated coherently. Figure 2 presents the maximal value of the conductance through resonant levels at $\epsilon_1-E_F=t_{12}$ and at $\epsilon_1-E_F=-|t_{12}|-(U_0+U_1-\Delta)/2$ as a function of the coulomb interaction parameter U_0. The height of both the peaks is equal to $2e^2/h$ at $U_0=0$ and rapidly drops for $U_0>\Gamma_\alpha$. The height of the one-electron peak (at $\epsilon_1-E_F=t_{12}$) is almost constant $(2e^2/h)\times(2/3)$ for larger U_0. The height of the two-electron peak monotonously decreases.

The conductance curve in Fig. 1 shows also a series of smaller conductance peaks, which correspond to transmission through excited electron states. The decoupling approximations used in the previous works[41–43] neglected such transmission channels. The dashed vertical lines in Fig. 1 show positions of resonant transmission through the one-electron states, whereas the solid lines—transmission through the two-electron states. Using the results from Table I Ione can assign the transmission channels at $\pm t_{12}+(U_0+U_1-\Delta)/2$ and $\pm t_{12}+U_1$ as through the singlet (s) and the triplet (t) states, respectively.

In the bottom part of Fig. 1 the correlators are presented: square of the local spin $\langle \mathbf{S}_i^2\rangle=\frac{3}{4}\langle(n_{i,+}-n_{i,-})^2\rangle$ and the correlator between the spins localized at both the dots $\langle \mathbf{S}_1\cdot\mathbf{S}_2\rangle=\frac{3}{4}\langle(n_{1,+}-n_{1,-})(n_{2,+}-n_{2,-})\rangle$. Using these correlators one can express square of the total spin $\langle(\mathbf{S}_1+\mathbf{S}_2)^2\rangle=\langle \mathbf{S}_1^2\rangle+\langle \mathbf{S}_2^2\rangle+2\langle \mathbf{S}_1\cdot\mathbf{S}_2\rangle$. The dependence of $\langle \mathbf{S}_i^2\rangle$ is similar to $\langle n_{i,\sigma}\rangle$ and its value increases when the gate voltage shifts ϵ_i below E_F. One can see that $\langle \mathbf{S}_i^2\rangle$ saturates passing the singlet state (at $\epsilon_1-E_F=-1.827$) in order to increase once again passing the triplet state (at $\epsilon_1-E_F=-2.6$). The maximal value of $\langle \mathbf{S}_i^2\rangle$ is achieved in the middle of the plot and it is closed to $\frac{3}{4}$—square of a spin of a free electron. The correlator $\langle \mathbf{S}_1\cdot\mathbf{S}_2\rangle$ is negative in the whole range, what indicates an antiferromagnetic coupling between the spins. The value of $-\langle \mathbf{S}_1\cdot\mathbf{S}_2\rangle$ increases at the singlet state and decreases passing the triplet

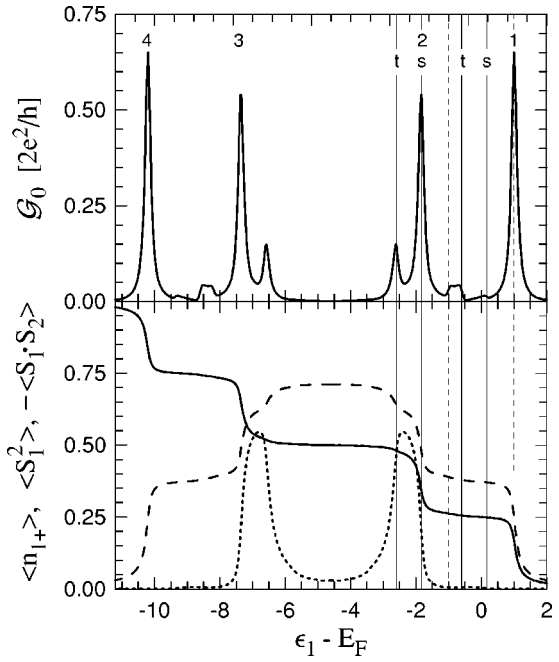

FIG. 1. Zero-voltage conductance $\mathcal{G}_0$ (top figure) and correlators (bottom figure): $\langle n_{1,+}\rangle$—solid curve, $\langle \mathbf{S}_1^2\rangle$—long-dashed curve, $-\langle \mathbf{S}_1\cdot\mathbf{S}_2\rangle$—short-dashed curve, as a function of the relative position of the energy level $\epsilon_1 - E_F$. The parameters are $t_{12}=1$, $U_0=6$, $U_1=1.6$, $\Gamma_L=\Gamma_R=0.1$, $\epsilon_2=\epsilon_1$, and $T=0$. The labels above the conductance peaks denote the position when an extra electron is added to the 2qd system. The vertical solid lines show positions of poles of the Green functions corresponding to transmission through the two-electron states: singlet (s) and the triplet (t), whereas the dashed lines—transmission through the one-electron states.

state. The length of the total spin is strongly reduced and achieves its minimal value $\langle(\mathbf{S}_1+\mathbf{S}_2)^2\rangle=0.2$. Note also a small bump in the spin correlation, which occurs between the singlet and the triplet state in the range $-0.6<\epsilon_1-E_F<0.173$. When the Fermi energy E_F lies between the one-electron state and the singlet state, there is one electron on average in the 2qd system with a local uncorrelated spin, which due interactions with conduction electrons can lead to

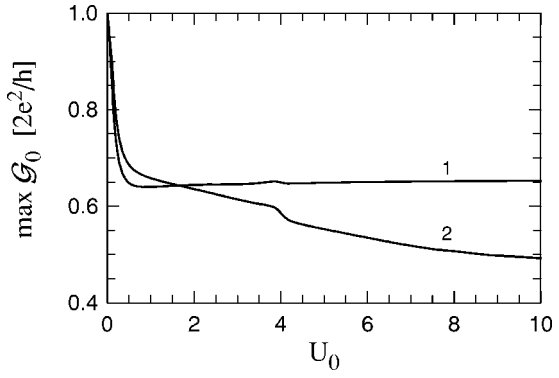

FIG. 2. Height of the conductance peaks through: (1) the one-electron level $\epsilon_1-E_F=|t_{12}|$ and (2) the singlet level $\epsilon_1-E_F=-|t_{12}|-(U_0+U_1-\Delta)/2$, plotted as the function of the intradot coulomb repulsion parameter U_0. The interdot coulomb interaction is taken $U_1=U_0/4$, $\Gamma_L=\Gamma_R=0.1$, $\epsilon_2=\epsilon_1$.

the Kondo resonance. When E_F passes the position of the singlet state we have double electron occupancy with the strong antiferromagnetic coupling between the local spins. Square of the total spin $\langle(\mathbf{S}_1+\mathbf{S}_2)^2\rangle$ is strongly compensated, which destroys the condition for the Kondo resonance. However, when the triplet state starts to participate in transport the antiferromagnetic correlations are much weaker. At $\epsilon_1-E_F=-4.6$ square of the total spin $\langle(\mathbf{S}_1+\mathbf{S}_2)^2\rangle=1.36$, which is a bit below the value 1.5 for square of the total spin of two free electrons. One can expect also strong fluctuations of the magnetic moment.

An interesting problem which arises is screening of the magnetic moment by conduction electrons in the 2qd system when the temperature T is lowered below T_K. Does the Kondo resonance appear for the 2qd system with two electrons, and what is a role of many-particle states in the effect? The effect could occur in a central part of Fig. 1, which can be achieved in an experiment for a very wide range of the gate voltage (even for moderate Coulomb interactions). According to our best knowledge the effect has not been studied experimentally in the 2qd system. A similar situation was predicted theoretically by Izumida *et al.*[39] and Hofstetter and Schoeller[40] for a multilevel quantum dot, which was just recently verified experimentally by Kogan *et al.*[50] For an odd number of electrons in the system they observed a peak in the source-drain conductance plot at $V=0$, which is a characteristic feature of the Kondo resonance. The similar feature was found for an even number of electrons, but the Kondo resonance range was separated by the gate voltage range between the singlet and the triplet state without the zero-voltage peak.[50] This is very similar to our situation discussed above. Pustilnik and Glazman[37] proposed an alternative scenario for two coupled electrons with $S=1$ suggesting a nonconventional Kondo resonance—in contrast to our model, in which the total magnetic moment is a composition of two spins of free electrons with a weak antiferromagnetic coupling.

Figure 3 shows dependence of the conductance spectrum on the coupling Γ_α. The height of the main peaks is almost constant, but the smaller peaks (related to transmission through excited states) depend on the coupling strength and their hight is proportional to Γ_α. The conductance peaks are asymmetrical, what is clearly seen for the peaks at $\epsilon_1-E_F=-1$ and -0.6. The asymmetry is related with interference processes. The current formula (5) has two terms: the first one is proportional to the local electron density of states (DOS) $\mathrm{Im}[\langle\langle c_{1,\sigma}|c_{1,\sigma}^\dagger\rangle\rangle_\omega^a]$ and the second—proportional to $\langle\langle c_{1,\sigma}|c_{1,\sigma}^\dagger\rangle\rangle_\omega^<$, which corresponds to interference processes. The interference term of the conductance is plotted in Fig. 3 as the dashed curve. These results show that for multi dot systems the local DOS as well as interference play an important role in transport and the formula (5) in its full form should be taken for calculations.

The results presented earlier are determined for the temperature $T=0$, because this case is much simpler for numerical calculations. On the other side, our approach is reliable for high temperatures $T>T_K$. The zero-temperatures studies can be a good qualitative description of the high temperature situation, and features of electronic transport presented above

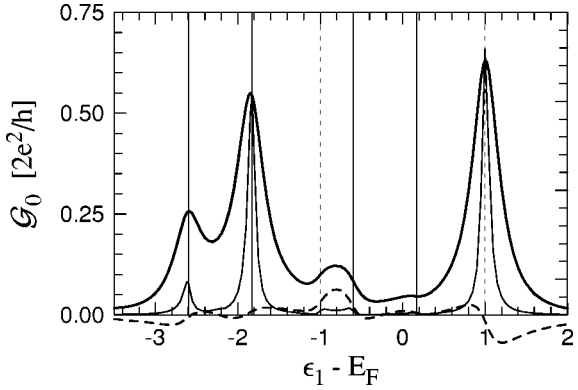

FIG. 3. Zero-voltage conductance $\mathcal{G}_0$ vs $\epsilon_1 - E_F$ for two different couplings of the 2qd system with the electrodes $\Gamma_L = \Gamma_R = 0.2$ (thick curve) and $\Gamma_L = \Gamma_R = 0.05$ (thin curve). The other parameters are the same as in Fig. 1. The dashed curve is the conductance determined form Eq. (5) taking only the interference term (the second one) for $\Gamma_L = \Gamma_R = 0.2$. Vertical lines denote position of resonant levels for the two-electron states (solid lines) and for the one-electron states (dashed lines).

survive in a wide temperature range. The procedure for a finite T is analogous to the $T=0$ case, in which one solves a set of integral equations for the thermal average of correlators. Figure 4 presents the dependence of $\mathcal{G}_0$ on ϵ_1 for different temperatures. As one could expect, the conductance peaks are smeared out, and significant changes are seen when $k_B T \approx \Gamma_\alpha$. Even at $k_B T = \Gamma_\alpha$ the triplet peak at $\epsilon_1 - E_F = -2.6$ is clearly seen as the shoulder of the peak at -1.827 (see the dashed curve). The conductance spectrum between the one-electron and two-electron resonance peaks changes slightly (see the peaks at -1, -0.6, and 0.17). These conductance peaks come from tails of the one-electron and the two-electron spectrum (at $\epsilon_1 - E_F = 1$ and at -1.827). Temperature changes of the tails are much smaller than changes at the resonance centers. For higher temperatures the smearing effect can be large enough and one can observe an increase of the electron density of states in the tails, which can result in an increase of the conductance as well (see the dot curve in

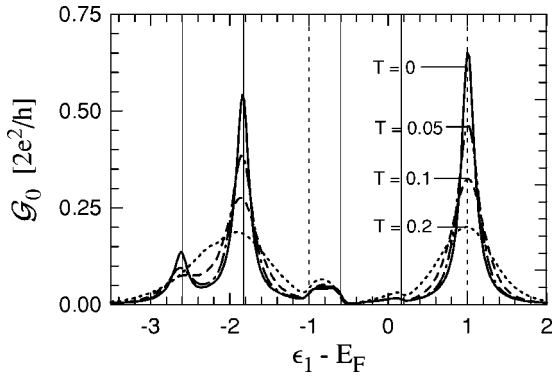

FIG. 4. Zero-voltage conductance $\mathcal{G}_0$ as a function of $\epsilon_1 - E_F$ for different temperatures: $T=0$—solid curve, $T=0.05$—dashed-dot curve, $T=0.1$—dashed curve, and $T=0.2$—dot curve. The coupling to the electrodes is $\Gamma_L = \Gamma_R = 0.1$, $t_{12}=1$, $U_0=6$, $U_1=1.6$, and $\epsilon_2 = \epsilon_1$.

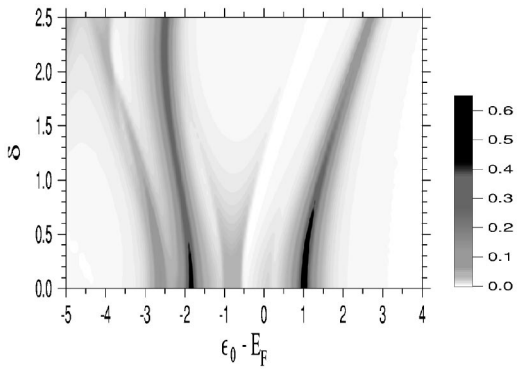

FIG. 5. Zero-voltage conductance $\mathcal{G}_0$ vs the center level position $\epsilon_0 = (\epsilon_1 + \epsilon_2)/2$ (with respect to E_F) and the detuning parameters $\delta = (\epsilon_1 - \epsilon_2)/2$ plotted as a gray-scale map. The parameters are $t_{12} = 1$, $U_0 = 6$, $U_1 = 1.6$, $\Gamma_L = \Gamma_R = 0.1$, and $T=0$.

Fig. 4 corresponding to $k_B T = 2\Gamma_\alpha$). The correlators are less sensitive to temperature changes than the conductance, because they are dependent on the Fermi distribution function whereas the conductance is dependent on its derivative. For example, in the center of the Hubbard gap $\epsilon_1 - E_F = -4.6$ square of the total spin $\langle (\mathbf{S}_1 + \mathbf{S}_2)^2 \rangle \approx 1.36$ for the temperatures up to $k_B T = 2\Gamma_\alpha$, the antiferromagnetic correlations are a bit reduced and the minimal value of $\langle (\mathbf{S}_1 + \mathbf{S}_2)^2 \rangle = 0.22$ at $k_B T = \Gamma_\alpha$ increases to 0.31 for $k_B T = 2\Gamma_\alpha$.

Applying a gate voltage different for each quantum dot one can shift the position of the energy levels ϵ_1 and ϵ_2. With the shift of the position of the resonant energies the conductance peaks change their height. The gray-scale plot of $\mathcal{G}_0$ is presented in Fig. 5 as a function of the average position of the levels $\epsilon_0 = (\epsilon_1 + \epsilon_2)/2$ and the detuning parameter $\delta = (\epsilon_1 - \epsilon_2)/2$. At $\delta = 0$, Fig. 5 shows the situation as in Fig. 1. Increasing δ the main conductance peaks are shifted from each other. The height of the single-electron conductance peak (at $\epsilon_0 - E_F = 1$ for $\delta = 0$) monotonously decreases with δ. The similar dependence has been observed experimentally[14,16,17] and calculated for coherent transport of noninteracting electrons.[20] The position of the one-electron states is given by

$$E_{1\pm} = \epsilon_0 \pm \sqrt{\delta^2 + t_{12}^2}. \tag{13}$$

The second large peak in Fig. 5 (at $\epsilon_0 - E_F = -1.827$ for $\delta = 0$) corresponds to two-electron singlet state and its height decreases much slower. The positions of the conductance peaks corresponding to the singlets are given as $E_{2\mathrm{Sn}} - E_{1\pm}$, where the singlet eigenenergies

$$E_{2\mathrm{Sn}} = 2\epsilon_0 + \frac{2U_0 + U_1}{3} + \frac{2}{3}\sqrt{p}\cos\left(\frac{\phi + 2\pi n}{3}\right) \quad \text{for } n = 0,1,2. \tag{14}$$

Here, we denoted $\phi = \arccos(q/p^{3/2})$, $p = (U_0 - U_1)^2 + 12\delta^2 + 12t_{12}^2$ and $q = (U_0 - U_1)[(U_0 - U_1)^2 + 18t_{12}^2 - 36\delta^2]$. The position of the conductance peak for the triplet state is $E_{2T} - E_{1\pm}$, where $E_{2T} = 2\epsilon_0 + U_1$. The small peaks at $\epsilon_0 - E_F = 0.173$, -0.6, and -1 from Fig. 1 are seen also in the gray plot in Fig. 5, but they disappear at large δ. Note that the

position of two-electron singlet level and the antibonding one-electron level (those at −1.827 and −1 for $\delta=0$) is shifted to the left-hand side in contrast to the bonding one-electron level, which is shifted to the right-hand side. The triplet state (at −2.6 for $\delta=0$) is well seen even for a large δ.

The results presented earlier are for moderate values of the coulomb parameters U_0 and U_1, for which the one- and the two-electron states are well separated from the three- and four-electron states (the Hubbard gap is large in our case). Moreover, we assumed a large electron transfer between the dots $t_{12} \gg \Gamma_\alpha$, for which the singlet and the triplet states are also well separated. For larger values of U_0, U_1 the difference between the position of the singlet and the triplet states is $J=16t_{12}^2/(U_0-U_1)$. When the coupling strength $\Gamma_\alpha > J$, the corresponding two conductance peaks merge together and specific features of the singlet and the triplet state are lost. The conductance spectrum is then similar to that for the incoherent sequential transport. Such the situation ($U_0 \to \infty$ and $J \to 0$) is often considered in the literature (see, e.g., Refs. 24–27 and 36).

B. Nonequilibrium transport

Let us now consider the nonequilibrium situation with a finite source-drain voltage drop V. Experimentally one can apply either the potential $V/2$ and $-V/2$ to the left and the right electrodes, or the potential V to the left electrode and in the right electrode the potential becomes zero. We choose the latter situations, which seems to be simpler for presentation. In the present studies full screening of the electric field on the quantum dots is assumed and the energy levels ϵ_i are independent on V. (The results presented later can be easily extended for the case when ϵ_i are shifted with increasing V.) Moreover, the approximation for the splitting of the Green functions keeps the poles at the same positions. Therefore, sweeping the potential V of the left electrode one can scan the electronic spectrum of the 2qd system.

Figure 6 presents the differential conductance $\mathcal{G}$ (the thick solid curve) when the levels $\epsilon_1-E_F=\epsilon_2-E_F=2$ are below the one-electron ground state and the 2qd systems is empty at the equilibrium (at $V=0$). For comparison the zero-voltage conductance $\mathcal{G}_0$ is plotted versus ϵ_1-E_F (see the thin solid curve). For the nonequilibrium situation four high conductance peaks are seen (in contrast to two peaks at the equilibrium). A large peak arises at $eV=3$, which is due to an activation of transmission through the one-electron antibonding state. The first peak (at $eV=1$ and corresponding to transmission through the one-electron bonding state) is also higher than that one at equilibrium. One can observe a large enhancement of the peak at $eV=4.6$ corresponding to transfer through the triplet state, whereas the singlet channel (at $eV=2.827$) gives a smaller value of $\mathcal{G}$. The peaks at $eV=1.827$ and $eV=2.6$ are a bit stronger.

The bottom part of Fig. 6 presents the voltage dependence of the correlators. The local occupancy $\langle n_{i,\sigma}\rangle$ is different for the first and the second dot (see the solid curves). An electronic polarization effect appears in the system. In the low voltage region (up to $eV \approx 2$) the polarization is negative and for large voltages the polarization is positive according the

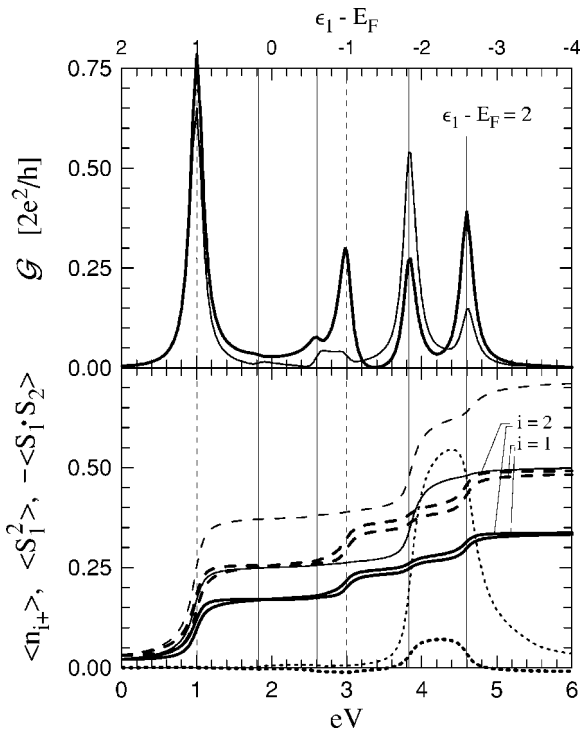

FIG. 6. Differential conductance $\mathcal{G}$ (top figure) and correlators (bottom figure): $\langle n_{i,+}\rangle$—solid curve, $\langle \mathbf{S}_i^2\rangle$—long-dashed curve, $-\langle \mathbf{S}_1\cdot\mathbf{S}_2\rangle$—short-dashed curve, as a function of the applied source-drain voltage V at $\epsilon_1-E_F=\epsilon_2-E_F=2$. Note that in the low voltage region the values of $\langle n_{i,+}\rangle$ and $\langle S_i^2\rangle$ for $i=1$ are larger than those ones for $i=2$, whereas in the high voltage regime the situation is opposite and these quantities are higher for $i=2$. The parameters are $t_{12}=1$, $U_0=6$, $U_1=1.6$, $\Gamma_L=\Gamma_R=0.1$, and $T=0$. For comparison the plot for the equilibrium situation is presented by the thin curves for the zero-voltage conductance $\mathcal{G}_0$ and the correlators as a function of ϵ_1-E_F (the top axis).

electric field. This result is in qualitative agreement with the Hartree-Fock approach used for the similar model,[51] where the polarization changed its sign and increased when the second transmission channel became activated in transport. The electron occupancy (in Fig. 6) saturates when the voltage passes the first resonance level, but its value is smaller than for the equilibrium case. This is not surprising, because electrons flow from the left electrode into the 2qd system and simultaneously flow out to the right electrode. The local electron occupancy depends on the Wigner distribution function, which is a combination of the Fermi distribution functions for both the electrodes. Therefore, when the chemical potential of the electrode passes the local energy levels of the system, one can observe steps of the charge accumulation with a fractional height. The voltage dependence of $\langle n_{i,\sigma}\rangle$ shows two additional steps at $eV=3$ and at $eV=4.6$, i.e., when a large activation of the conducting channels occur. Square of the local spins $\langle \mathbf{S}_i^2\rangle$ increase with V and their dependences are similar to the local charge $\langle n_{i,\sigma}\rangle$. The short-dashed curves in bottom of Fig. 6 represent the correlator $-\langle \mathbf{S}_1\cdot\mathbf{S}_2\rangle$ for the nonequilibrium and the equilibrium situation. The strong antiferromagnetic correlations at the singlet state are reduced substantially when a high source-drain volt-

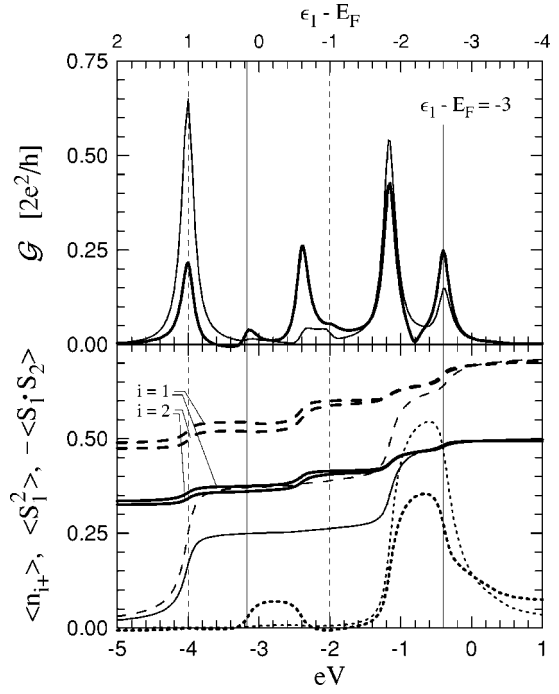

FIG. 7. Differential conductance $\mathcal{G}$ (top figure) and correlators (bottom figure): $\langle n_{i,+}\rangle$—solid curve, $\langle \mathbf{S}_i^2\rangle$—long-dashed curve, $-\langle \mathbf{S}_1\cdot\mathbf{S}_2\rangle$—short-dashed curve, as a function of the applied source-drain voltage V at $\epsilon_1-E_F=\epsilon_2-E_F=-3$. The parameters are $t_{12}=1$, $U_0=6$, $U_1=1.6$, $\Gamma_L=\Gamma_R=0.1$. For comparison the plot for the equilibrium situation is presented by the thin curves for the zero-voltage conductance $\mathcal{G}_0$ and correlators as a function of ϵ_1-E_F (the top axis).

age is applied. Moreover, some small ferromagnetic correlations are found (at $eV\approx 3$ and $eV\approx 6$). These results suggest that flowing currents reduce antiferromagnetic correlations.

Figure 7 shows the same quantities as in Fig. 6, now, for $\epsilon_1-E_F=\epsilon_2-E_F=-3$, i.e., for double electron occupancy at the equilibrium. In this case a negative voltage V is used to scan the conductance spectrum. Once again four significant peaks of $\mathcal{G}$ are seen. In this case a strongest activation exhibits the triplet channel at $eV=-2.4$. The one-electron channel transmission is much weaker and the corresponding conductance peak (at $eV=-4$) is much lower than the peak at the equilibrium. Changes of the peaks for the singlet and the triplet channels (at $eV=-1.287$ and $eV=-0.4$) are not so large as in Fig. 6. The electronic charge $\langle n_{i,\sigma}\rangle$ decreases and one can see steps at the same position as for the high conduction peaks. The polarization effect occurs for this case as well. For small voltages the polarization is opposite to the electric field, in order to change its orientation for a high voltage drop ($eV<-2$). The spin correlations $\langle \mathbf{S}_1\cdot\mathbf{S}_2\rangle$ are reduced, although not so strong as in Fig. 6. One finds antiferromagnetic correlations again in the range $-3.173<eV<-2.4$, which may be related to proximity of the excited singlet channel.

IV. SUMMARY

In this work theoretical studies of coherent electronic transport in the system of two coupled dots connected in series with electrodes were performed within the two-impurity Anderson model taking into account the intra- and the interdot coulomb interactions. The conductance characteristics were determined by means of the nonequilibrium Green function technique using the equation of motion approach, in which all correlations inside the 2qd system were treated exactly and a decoupling procedure for the Green function connecting the 2qd system with the electrodes was applied. Although the procedure neglects spin fluctuations, it takes into account charge fluctuations. Therefore, it is reliable for temperatures higher than the Kondo temperature T_K and for any value of the source-drain voltage V, also for large V.

Our attention was focused on electronic correlations, formation of many-body states and their role in transport. The analysis was done for the system of strongly coupled dots, in which the interdot electron transfer is large $t_{12}>\Gamma_\alpha$ and with moderate Coulomb interactions $U_0>U_1>t_{12}$. In this case the singlet and the triplet state are well separated, which gives a good opportunity for analysis of transport through these states. The analysis of the conductance was performed as a function of the position of the dot levels ϵ_i shifted by the gate voltage and for nonequilibrium as a function of the source-drain voltage (at the constant position of ϵ_i). Apart from the resonance peaks a significant contribution to transport through excited many-particle states was found. The triplet states give the significant contribution to the conductance and we predict that this should be a measurable effect in a wide range of temperatures. In the present procedure all many-body correlators were determined in a self-consistent way. A detailed analysis of the spin-spin correlation function showed an antiferromagnetic coupling connected with a formation of the singlet state, for which the total magnetic moment is strongly compensated. However, when the triplet state starts to participate in transport the antiferromagnetic coupling is reduced, the spins are loosely coupled and strongly fluctuate. Such the situation occurs in a wide range of the gate voltages when the Fermi energy lies in the Hubbard gap and in a wide range of temperatures, provided that the on-site Coulomb repulsion is strong enough ($U_0>2|t|$ for $U_1=0$) and the energy splitting between the lowest singlet state and the triplet state is relatively small. Note, however, that in an improved treatment of the model one can expect a quantitative modification of the observed tendency to suppression of the spin-spin correlations in the lowest temperatures, where the (neglected here) correlations responsible for the Kondo effect become important.

For the nonequilibrium situation the procedure kept the position of the poles of the Green functions and therefore, sweeping the source-drain voltage one scans the electronic spectrum of the system. The conductance characteristics obtained in this way showed a strong activation of the transmission through excited states with the conductance peaks so high as the resonant peaks. The activation of the channels depended on the equilibrium position of the system. For an empty system (with the energy levels $\epsilon_i \gg E_F$) at the equilibrium the conductance corresponding to the one-electron states was strongly enhanced, whereas for the system with two electrons at $V=0$ (ϵ_i-E_F in the Hubbard gap) the triplet states were activated for the large voltages. As one could

expect, the analysis showed smaller spin-spin correlations and a reduction of the antiferromagnetic coupling.

The main drawback of the approach used here is the neglect of electron correlations leading to the Kondo effect what limits our results to $T > T_K$ range. Within the framework of the EOM method one can try to extend our work to low-T regime, by taking into account electron correlators involving both the lead and the 2qd degrees of freedom at the same time, following the approach presented by Lacroix.[52] One should be aware, however, the enormous complications which would arise in the present case due to necessity of treatment of the large number of correlators on equal footing in order to keep the proportions between the various excitation processes.

Although the address of the present work is to the system of the two quantum dots, the same model can be used for studies of transport through single molecules. As an example let it be the (N,N′,N″-trimethyl-1,4,7-triazacyclononane)$_2$-$V_2(CN)_4$(μ-C_4N_4) molecule, which was used recently by Liang *et al.*[7] for the conductance measurements. The molecule contains two vanadium centers, and therefore, it can be described by the same model.

ACKNOWLEDGMENTS

The authors would like to thank Arturo Tagliacozzo for his helpful discussions. This work was supported by the State Committee for Scientific Research (Poland) Project No. PBZ KBN 044 P03 2001.

APPENDIX: SINGLE-DOT CASE

Let us present the decoupling procedure for the Green functions for the case of the single dot. The calculations are much simpler and one can see better the approximations made during this procedure. From the EOM one finds the retarded single-particle and the two-particle Green functions at the dot as

$$(\omega-\epsilon_1)\langle\langle c_{1,\sigma}|c^\dagger_{1,\sigma}\rangle\rangle^r_\omega = 1+\sum_\alpha t_\alpha\sum_k\langle\langle c_{k\alpha,\sigma}|c^\dagger_{1,\sigma}\rangle\rangle^r_\omega + U\langle\langle c_{1,\sigma}n_{1,-\sigma}|c^\dagger_{1,\sigma}\rangle\rangle^r_\omega, \tag{A1}$$

$$\begin{aligned}(\omega-\epsilon_1-U)\langle\langle c_{1,\sigma}n_{1,-\sigma}|c^\dagger_{1,\sigma}\rangle\rangle^r_\omega &= \langle n_{1,-\sigma}\rangle+\sum_\alpha t_\alpha\sum_k[\langle\langle c_{k\alpha,\sigma}n_{1,-\sigma}|c^\dagger_{1,\sigma}\rangle\rangle^r_\omega \\ &-\langle\langle c_{1,\sigma}c^\dagger_{k\alpha,-\sigma}c_{1,-\sigma}|c^\dagger_{1,\sigma}\rangle\rangle^r_\omega \\ &+\langle\langle c_{1,\sigma}c^\dagger_{1,-\sigma}c_{k\alpha,-\sigma}|c^\dagger_{1,\sigma}\rangle\rangle^r_\omega].\end{aligned} \tag{A2}$$

In the second step of the EOM one finds

$$\sum_k\langle\langle c_{k\alpha,\sigma}|c^\dagger_{1,\sigma}\rangle\rangle^r_\omega = t_\alpha g^r_\alpha(\omega)\langle\langle c_{1,\sigma}|c^\dagger_{1,\sigma}\rangle\rangle^r_\omega, \tag{A3}$$

where $g^r_\alpha(\omega)$ is the retarded Green function in the α electrode, and which is taken as $g^r_\alpha(\omega)=\Sigma_k[1/(\omega-\epsilon_k+i0)] \approx -i\pi\rho_\alpha$. In Eq. (A2) for two-particle Green function we neglect the resonance broadening terms related to the simultanuous hopping of electron pairs to and out of the 2qd: $\langle\langle c_{1,\sigma}c^\dagger_{k\alpha,-\sigma}c_{1,-\sigma}|c^\dagger_{1,\sigma}\rangle\rangle^r_\omega$ and $\langle\langle c_{1,\sigma}c^\dagger_{1,-\sigma}c_{k\alpha,-\sigma}|c^\dagger_{1,\sigma}\rangle\rangle^r_\omega$ (the sum of these terms vanish in the Hartree-Fock decoupling), effectively closing the system of equations for the Green functions. In the case of the single-dot this procedure is equivalent to the one used by Pals and MacKinnon,[41] who showed that it compares favorably well with the results of approximation of Meir *et al.*,[53] and gives reliable results for $T > T_K$.[52] Note, however, that in the case of 2qd additional terms are generated by interdot hopping and the interaction, leading to appearance of novel interdot correlation functions. In the paper of Pals and MacKinnon[41] these correlation functions were decoupled in a mean-field way, whereas here we compute all such correlations selfconsistently using the Green functions.

For the case of the single-dot this approximation leads to the following retarded Green function:

$$\langle\langle c_{1,\sigma}|c^\dagger_{1,\sigma}\rangle\rangle^r_\omega = (1-\langle n_{1,-\sigma}\rangle)G^r_0(\omega)+\langle n_{1,-\sigma}\rangle G^r_U(\omega), \tag{A4}$$

where $\epsilon^r_1=\epsilon_1+i\Gamma$, $\Gamma=\Gamma_L+\Gamma_R$, $G^r_0(\omega)=1/(\omega-\epsilon^r_1)$, and $G^r_U(\omega)=1/(\omega-\epsilon^r_1-U_0)$. (Note the larger energy level broadening for the single-dot system than for two quantum dots.) Using the symmetrization procedure from Sec. II one derives the lesser Green function as

$$\langle\langle c_{1,\sigma}|c^\dagger_{1,\sigma}\rangle\rangle^<_\omega = 2if_1(\omega)\{(1-\langle n_{1,-\sigma}\rangle)\mathrm{Im}[G^r_0]+\langle n_{1,-\sigma}\rangle\mathrm{Im}[G^r_U]\}, \tag{A5}$$

where $f_1(\omega)=\gamma_L f_L(\omega)+\gamma_R f_R(\omega)$ and $\gamma_\alpha=\Gamma_\alpha/\Gamma$. The local density of electrons is expressed by

$$\begin{aligned}\langle n_1\rangle &= \sum_\sigma\langle n_{1,\sigma}\rangle \equiv \sum_\sigma\int\frac{d\omega}{2i\pi}\langle\langle c_{1,\sigma}|c^\dagger_{1,\sigma}\rangle\rangle^<_\omega \\ &= \left(1-\frac{\langle n_1\rangle}{2}\right)\eta_0+\frac{\langle n_1\rangle}{2}\eta_U,\end{aligned} \tag{A6}$$

where $\eta_\nu=\int d\omega f_1(\omega)\mathrm{Im}[G^r_\nu]/\pi$ is the occupancy of uncorrelated electrons at the energy level $E_{\nu=0}=\epsilon_1$ and $E_{\nu=U}=\epsilon_1+U_0$. It is useful to introduce the function

$$\begin{aligned}F(\mu_\alpha-E_\nu) &\equiv \int\frac{d\omega}{\pi}f_\alpha(\omega)\mathrm{Im}[G^r_\nu] \\ &= 1+\frac{2}{\pi}\,\mathrm{Im}\left[\Psi\left(\frac{1}{2}-\frac{\mu_\alpha-E_\nu-i\Gamma}{2\pi ik_BT}\right)\right],\end{aligned} \tag{A7}$$

where Ψ the digamma function. At the temperature $T=0$ this function is simply expressed as $F^0(\mu_\alpha-E_\nu)=1+(2/\pi)$ arc $\tan[(\mu_\alpha-E_\nu)/\Gamma]$. Therefore, $\eta_\nu=\Sigma_\alpha\,\gamma_\alpha F(\mu_\alpha-E_\nu)$ and from Eq. (6) one gets $\langle n_1\rangle=2\eta_0/(2+\eta_0-\eta_U)$.

Inserting Eqs. (A4) and (A5) into (5) one gets the current

$$I=\left(1-\frac{\langle n_1\rangle}{2}\right)I_0+\frac{\langle n_1\rangle}{2}I_U, \tag{A8}$$

where

$$I_\nu = \frac{e}{\hbar}\frac{4\Gamma_L\Gamma_R}{\Gamma}\int \frac{d\omega}{\pi}[f_R(\omega) - f_L(\omega)]\mathrm{Im}[G^r_\nu] \qquad \text{(A9)}$$

for $\nu=0$, U. Using (A7) one can express

$$I_\nu = \frac{2e}{h}\frac{8\Gamma_L\Gamma_R}{\Gamma}\mathrm{Im}\left[\Psi\left(\frac{1}{2} - \frac{\mu_R - E_\nu - i\Gamma}{2\pi i k_B T}\right) - \Psi\left(\frac{1}{2} - \frac{\mu_L - E_\nu - i\Gamma}{2\pi i k_B T}\right)\right]. \qquad \text{(A10)}$$

The conductance can be derived as

$$\mathcal{G} = \left(1 - \frac{\langle n_1\rangle}{2}\right)\mathcal{G}_0 + \frac{\langle n_1\rangle}{2}\mathcal{G}_U + (I_U - I_0)\frac{\partial\langle n_1\rangle}{2\partial V}, \qquad \text{(A11)}$$

where $\mathcal{G}_\nu$ is the conductance of uncorrelated electrons through the energy level E_ν. Assuming the chemical potentials in the electrodes $\mu_R = E_F + eV$ and $\mu_L = E_F$ one can express $\mathcal{G}_\nu$ as

$$\mathcal{G}_\nu = \frac{2e^2}{h}\frac{8\Gamma_L\Gamma_R}{2\pi k_B T\Gamma}\mathrm{Re}\left[\Psi'\left(\frac{1}{2} - \frac{E_F + eV - E_\nu - i\Gamma}{2\pi i k_B T}\right)\right], \qquad \text{(A12)}$$

where Ψ' denotes the derivative of the digamma function. At $T=0$ it is simply

$$\mathcal{G}_\nu = \frac{2e^2}{h}\frac{4\Gamma_L\Gamma_R}{(E_F + eV - E_\nu)^2 + \Gamma^2}. \qquad \text{(A13)}$$

In the zero-voltage limit the conductance reaches its maximal value at the resonances E_ν. The average number of electrons is $\langle n_1\rangle = 2/3$ at E_0 and $\langle n_1\rangle = 4/3$ at E_U. It means that within our decoupling procedure the conductance peaks can reach the value $\max\{\mathcal{G}\} = (2/3)\times(2e^2/h)$. For larger voltages also the last term of (A11) plays a role and it can change the height of the conductance peaks.

[1] D. Goldhaber-Gordon, H. Shtrikman, D. Mahalu, D. Abusch-Magder, U. Meirav, and M. A. Kastner, Nature (London) **391**, 56 (1998); D. Goldhaber-Gordon, J. Gores, M. A. Kastner, H. Shtrikman, D. Mahalu, and U. Meirav, Phys. Rev. Lett. **81**, 5225 (1998).

[2] See, e.g., L. Kouwenhoven and L. I. Glazman, Phys. World **14**, 33 (2001), and references therein.

[3] J. Gores, D. Goldhaber-Gordon, S. Heemeyer, M. A. Kastner, H. Shtrikman, D. Mahalu, and U. Meirav, Phys. Rev. B **62**, 2188 (2000).

[4] J. Nygard, D. H. Cobden, and P. E. Lindelof, Nature (London) **408**, 342 (2000).

[5] W. Liang, M. Bockrath, D. Bozovic, J. H. Hafner, M. Tinkham, and H. Park, Nature (London) **411**, 665 (2001); W. Liang, M. Bockrath, and H. Park, Phys. Rev. Lett. **88**, 126801 (2002).

[6] H. C. Monoharan, C. P. Lutz, and D. M. Eigler, Nature (London) **403**, 512 (2000).

[7] W. J. Liang, M. P. Shores, M. Bockrath, J. R. Long, and H. Park, Nature (London) **417**, 725 (2002).

[8] J. Park, A. N. Pasupathy, J. I. Goldsmith, C. Chang, Y. Yaish, J. R. Petta, M. Rinkoski, J. P. Sethna, H. D. Abruna, P. L. McEuen, and D. C. Ralph, Nature (London) **417**, 722 (2002).

[9] D. Loss and D. P. Di Vincenzo, Phys. Rev. A **57**, 120 (1998).

[10] R. H. Blick, D. Pfannkuche, R. J. Haug, K. v. Klitzing, and K. Eberl, Phys. Rev. Lett. **80**, 4032 (1998).

[11] A. W. Holleitner, C. R. Decker, H. Qin, K. Eberl, and R. H. Blick, Phys. Rev. Lett. **87**, 256802 (2001).

[12] A. W. Holleitner, R. H. Blick, A. K. Huttel, K. Eberl, and J. P. Kotthaus, Science **297**, 70 (2002).

[13] M. C. Rogge, C. Fuhner, U. F. Keyser, R. J. Haug, M. Bichler, G. Abstreitere, and W. Wegscheider, Appl. Phys. Lett. **83**, 1163 (2003).

[14] H. Jeong, A. M. Chang, and M. R. Melloch, Science **293**, 2221 (2001).

[15] H. Qin, A. W. Holleitner, K. Eberl, and R. H. Blick, Phys. Rev. B **64**, 241302 (2001).

[16] M. Pioro-Ladriere, M. Ciorga, J. Lapointe, P. Zawadzki, M. Korkusiński, P. Hawrylak, and A. S. Sachrajda, Phys. Rev. Lett. **91**, 026803 (2003).

[17] T. Hayashi, T. Fujisawa, H. D. Cheong, Y. H. Jeong, and Y. Hirayama, Phys. Rev. Lett. **91**, 226804 (2003).

[18] R. H. Blick, A. K. Huttel, A. W. Holleitner, E. M. Hohberger, H. Qin, J. Kirschbauma, J. Weber, W. Wegscheider, M. Bichler, K. Eberl, and J. P. Kotthaus, Physica E (Amsterdam) **16**, 76 (2003).

[19] M. Pustilnik, L. I. Glazman, D. H. Cobden, and L. P. Kouwenhoven, Lect. Notes Phys. **579**, 3 (2001).

[20] R. Ziegler, C. Bruder, and H. Schoeller, Phys. Rev. B **62**, 1961 (2000).

[21] K. Kawamura and T. Aono, Jpn. J. Appl. Phys., Part 1 **36**, 3951 (1997).

[22] V. Mujica, M. Kemp, A. Roitberg, and M. Ratner, J. Chem. Phys. **104**, 7296 (1996).

[23] A. Oguri, Phys. Rev. B **63**, 115305 (2001).

[24] T. Aono, M. Eto, and K. Kawamura, J. Phys. Soc. Jpn. **67**, 1860 (1998); Jpn. J. Appl. Phys., Part 1 **38**, 315 (1999); T. Aono and M. Eto, Phys. Rev. B **63**, 125327 (2001).

[25] A. Georges and Y. Meir, Phys. Rev. Lett. **82**, 3508 (1999).

[26] R. Aguado and D. C. Langreth, Phys. Rev. Lett. **85**, 1946 (2000); R. Lopez, R. Aguado, and G. Platero, *ibid.* **89**, 136802 (2002).

[27] P. A. Orellana, G. A. Lara, and E. V. Anda, Phys. Rev. B **65**, 155317 (2002).

[28] P. Coleman, Phys. Rev. B **29**, 3035 (1984); **35**, 5072 (1987).

[29] G. Klimeck, G. Chen, and S. Datta, Phys. Rev. B **50**, 2316 (1994).

[30] G. Chen, G. Klimeck, S. Datta, G. Chen, and W. A. Goddard III, Phys. Rev. B **50**, 8035 (1994).

[31] C. A. Stafford, Phys. Rev. Lett. **77**, 2770 (1996).

[32] Y. Tanaka and H. Akera, Phys. Rev. B **53**, 3901 (1996).

[33] R. Kotlyar and S. Das Sarma, Phys. Rev. B **56**, 13 235 (1997).

[34] Y. Asano, Phys. Rev. B **58**, 1414 (1998).

[35] W. G. van der Wiel, S. De Franceschi, J. M. Elzerman, T. Fujisawa, S. Tarucha, and L. P. Kowenhoven, Rev. Mod. Phys.

75, 1 (2003).
[36] R. Aguado and D. C. Langreth, Phys. Rev. B **67**, 245307 (2003).
[37] M. Pustilnik, Y. Avishai, and K. Kikoin, Phys. Rev. Lett. **84**, 1756 (2000); M. Pustilnik and L. I. Glazman, *ibid.* **85**, 2993 (2000); **87**, 216601 (2001); Phys. Rev. B **64**, 045328 (2001).
[38] D. Giuliano and A. Tagliacozzo, Phys. Rev. Lett. **84**, 4677 (2000); D. Giuliano, B. Jouault, and A. Tagliacozzo, Phys. Rev. B **63**, 125318 (2001).
[39] W. Izumida, O. Sakai, and S. Tarucha, Phys. Rev. Lett. **87**, 216803 (2001); O. Sakai and W. Izumida, Physica B **328**, 125 (2003).
[40] W. Hofstetter and H. Schoeller, Phys. Rev. Lett. **88**, 016803 (2002).
[41] P. Pals and A. MacKinnon, J. Phys.: Condens. Matter **8**, 5401 (1996).
[42] J. Q. You and H. Z. Zheng, Phys. Rev. B **60**, 13 314 (1999).
[43] S. Lamba and S. K. Joshi, Phys. Rev. B **62**, 1580 (2000).
[44] H. Haug and A.-P. Jauho, *Quantum Kinetics in Transport and Optics of Semiconductors* (Springer-Verlag, Berlin, 1998).
[45] D. K. Ferry, *Transport in Nanostructures* (Cambridge University Press, Cambridge, 1997).
[46] G. D. Mahan, Phys. Rep. **145**, 251 (1987).
[47] J. Rammer and H. Smith, Rev. Mod. Phys. **58**, 323 (1986).
[48] C. Niu, D. L. Lin, and T. H. Lin, J. Phys.: Condens. Matter **11**, 1511 (1999).
[49] A. B. Harris and R. V. Lange, Phys. Rev. **157**, 295 (1967).
[50] A. Kogan, G. Granger, M. A. Kastner, D. Goldhaber-Gordon, and H. Shtrikman, Phys. Rev. B **67**, 113309 (2003).
[51] T. Kostyrko and B. R. Bułka, Phys. Rev. B **67**, 205331 (2003).
[52] C. Lacroix, J. Phys. F: Met. Phys. **11**, 2389 (1981).
[53] Y. Meir, N. S. Wingreen, and P. A. Lee, Phys. Rev. Lett. **66**, 3048 (1991).